Published in final edited form as:
Oncogene. 2013 August 29; 32(35): 4064–4077. doi:10.1038/onc.2012.417.

Neurotrophin-3 modulates breast cancer cells and the microenvironment to promote the growth of breast cancer brain metastasis

E Louie, **XF Chen**, **A Coomes**, **K Ji**, **S Tsirka**, and **EI Chen**
Department of Pharmacological Sciences, Stony Brook University, Stony Brook, NY, USA

Abstract

Metastasis, which remains incompletely characterized at the molecular and biochemical levels, is a highly specific process. Despite the ability of disseminated cancer cells to intravasate into distant tissues, it has been long recognized that only a limited subset of target organs develop clinically overt metastases. Therefore, subsequent adaptation of disseminated cancer cells to foreign tissue microenvironment determines the metastatic latency and tissue tropism of these cells. As a result, studying interactions between the disseminated cancer cells and the adjacent stromal cells will provide a better understanding of what constitutes a favorable or unfavorable microenvironment for disseminated cancer cells in a tissue-specific manner. Previously, we reported a protein signature of brain metastasis showing increased ability of brain metastatic breast cancer cells to counteract oxidative stress. In this study, we showed that another protein from the brain metastatic protein signature, neurotrophin-3 (NT-3), has a dual function of regulating the metastatic growth of metastatic breast cancer cells and reducing the activation of immune response in the brain. More importantly, increased NT-3 secretion in metastatic breast cancer cells results in a reversion of mesenchymal-like (EMT) state to epithelial-like (MET) state and vice versa. Ectopic expression of NT-3 in EMT-like breast cancer cells reduces their migratory ability and increases the expression of HER2 (human epidermal growth factor receptor 2) and E-cadherin at the cell–cell junction. In addition, both endogenous and ectopic expression of NT-3 reduced the number of fully activated cytotoxic microglia. In summary, NT-3 appears to promote growth of metastatic breast cancer cells in the brain by facilitating the re-epithelialization of metastatic breast cancer cells and downmodulating the cytotoxic response of microglia. Most importantly, our results provide new insights into the latency and development of central nervous system macrometastases in patients with HER2-positive breast tumors and provide mechanistic rationale to target HER2 signaling for HER2-positive breast cancer brain metastasis.

Keywords

breast cancer; brain metastasis; neurotrophin-3; protein signature; HER2 positive; HER2 signaling

Correspondence: Dr EI Chen, Department of Pharmacological Sciences, Stony Brook University, BST 8-125, Stony Brook, NY 11794-8651, USA, emily@pharm.stonybrook.edu.

CONFLICT OF INTEREST
The authors declare no conflict of interest.

INTRODUCTION

For most types of cancer, including breast cancer, the development of on-going metastasis leads to clinically incurable disease. Much attention has been focused on what stimulates cancer cells to emigrate from primary tumors. Clinically relevant questions of metastasis such as why metastasis is highly inefficient and what are the determinants of tissue tropism for different cancer types remain unanswered. Breast cancer preferentially metastasizes to lymph nodes, bone, lung, brain and liver.[1–5] Brain metastases are an increasingly important cause of morbidity and mortality in breast cancer patients because of improved survival of cancer patients. Nearly 20% of breast cancer patients are eventually diagnosed with brain lesions, making breast cancer the main source of metastatic brain disease in women.[2,6–8] Owing to the lack of diagnostic markers, brain metastases remain undetected until they become symptomatic. Thus, brain metastases present a therapeutic challenge for the physician and an emotionally and physically debilitating event for the patient.

The brain is an organ with a specialized microenvironment different from other target organ sites of metastasis. Unlike most other organs, the neural tissue does not have significant extracellular spaces; this provides a highly compact space for neural functions combined with a restriction on unwanted cellular and molecular movements.[9] Unlike other organ-specific metastases, breast cancer brain metastases have an exceptionally long latency with a median latent time of 16 years after the initial diagnosis of breast cancer.[10–12] Therefore, we have been focusing on the cellular adaptation of brain metastatic breast cancer cells and the therapeutic implication of these adaptive mechanisms. To identify the determinants of breast cancer brain metastasis, we utilized large-scale mass spectrometry-based proteomics previously to identify a proteomic signature of differentially expressed proteins in metastatic breast cancer cells with a high propensity to colonize the brain as opposed to the bone or the initial disseminating cell.[13] Previously, we established a brain metastatic signature with ~20% of these proteins involved in oxidative phosphorylation.[13] In this study, we determined the role of another target protein from the brain metastatic signature in promoting the metastatic growth of breast cancer cells in the brain.

Neurotrophin-3 (NT-3) is a neurotrophic factor in the NGF (nerve growth factor) family of neurotrophins. Other members of the NGF family include NGF, brain-derived growth factor (BDNF) and neurotrophin-4/5 (NT-4/5). They activate two structurally unrelated receptors, the p75 neurotrophin receptor ($p75^{NTR}$) and the receptor tyrosine kinase designated TRK. The $p75^{NTR}$ binds all NTs with low affinity, whereas the Trk receptors show high-affinity binding to specific NTs.[14] Although members of the NGF family, such as NGF, BDNF and NT-4/5, have been reported to promote proliferation, survival and potentially metastasis of breast cancer cells,[15–18] the involvement of NT-3 in breast cancer metastasis, particularly breast cancer brain metastasis, has not been reported. As predicted by the proteomic signature, we found increased mRNA, protein and secretion of NT-3 in breast cancer cell lines capable of generating macroscopic lesions in the brain. We showed that NT-3 has a dual function of promoting the metastatic growth of breast cancer cells in the brain. First, NT-3 promotes the mesenchymal–epithelial transition (MET) of breast cancer cells to a more epithelial-like phenotype and dramatically enhances the ability of these reverted breast cancer cells to proliferate in the brain. Consequently, knocking down NT-3 in epithelial-like

breast cancer cells leads to partial reversion to epithelial–mesenchymal transition (EMT)-like phenotype and a dramatic reduction of metastatic tumor burden in the brain. Also, NT-3-induced mesenchymal–epithelial reversion coincides with reduced migratory ability, increased expression of HER2 (human epidermal growth factor receptor 2) and E-cadherin at the cell–cell junction and reduced expression of EMT-inducing transcription factor such as Snail in the MET reverted breast cancer cells.

Increased E-cadherin expression in metastases compared with the primary tumors has been reported in human patient specimens.[19,20] Furthermore, the importance of epithelial phenotype in the formation of secondary tumors has been demonstrated in different metastasis models, including bladder cancer,[21,22] prostate cancer,[23,24] colorectal cancer[25] and breast cancer.[20] In accordance with these findings, we found that EMT-like breast cancer cells (NT-3 low) displaying a more invasive phenotype *in vitro* yield only micrometastasis in the brain, whereas epithelial-like breast cancer cells (NT-3 high) displaying reduced invasive phenotype *in vitro* are able to proliferate and form macrometastasis in the brain. The EMT and MET status of breast cancer cells can also affect the response of immune cells in the brain. Glial cells have been reported to surround and infiltrate metastatic tumors in the brain.[26,27] Microglia are the main immunocompetent cells in the central nervous system (CNS), as most other inflammatory cells are excluded from the brain. However, microglia in metastatic lesions exhibit only low level of activation and appear to promote the growth of metastatic tumors in the brain instead of exerting cytotoxic effects.[26] In our studies, we found that EMT-like breast cancer cells appear to elicit rapid activation of microglial, suggesting that the innate immune response in the brain leads to the disappearance of these cells in the brain over time. In contrast, epithelial-like breast cancer cells elicit significantly lower microglia activation accompanied by proliferation of these cells in the brain over time. Manipulation of NT-3 secretion in breast cancer cells results in changes in the EMT status of breast cancer cells and the corresponding microglia response in the brain. Interestingly, NT-3 has been reported to inhibit microglia activation[28] and has both mitogenic and trophic effects on microglia.[27,29] Our findings are consistent with previously published effects of NT-3 on microglia, and suggest that NT-3 secreted by metastatic tumor cells can also modulate microglial functions. Together, our current results support the idea that the ability of disseminated cancer cells to undergo EMT and subsequent MET in the appropriate microenvironment is a key attribute for successful metastasis.

RESULTS

Increased expression of NT-3 in brain metastatic breast cancer cells

To confirm the specificity of NT-3 expression in brain metastatic breast cancer cells, we studied the transcriptional profile of NTs and their receptors in brain selective BCM2 BrainG2 and MDA-MB 361 breast cancer cell lines, and non-brain selective BCM2 and MDA-MB 231 breast cancer cell lines. BCM2 BrainG2 cells were isolated from the brains of mice injected with the BCM2 metastatic breast cancer cell line intravenously and were shown to form macrometastasis in the brain selectively.[13] MDA-MB 361 cells were established from brain metastasis of a breast cancer patient.[3] Both BCM2 and MDA-MB

361 exhibit more epithelial-like phenotype. On the contrary, BCM2 and MDA-MB 231 breast cancer cell lines were isolated from the plural effusion of breast cancer patients and exhibit mesenchymal-like (EMT-like) phenotype.[3,13] The mRNA expression of NTs (NT-3, NGF, BDNF and NT-4/5), Trks (TrkA, TrkB and TrkC) and $p75^{NTR}$ was quantified by real-time qPCR. As shown in Figure 1a, NT-3 mRNA level was significantly higher in both brain selective breast cancer cell lines, BCM2 BrainG2 (8.1-fold higher) and MDA-MB 361 (16-fold higher), compared with the non-brain selective breast cancer cell lines, BCM2 and MDA-MB 231. On the contrary, NGF, BDNF and NT-4/5 mRNA levels were lower in the brain selective cell lines than the non-brain selective breast cancer cell lines (Figure 1a). For Trk receptor expression, we found low TrkA and slightly increased TrkC mRNAs in brain selective breast cancer cell lines compare with the non-brain selective breast cancer cell lines. TrkB mRNA was below the detection limit in all cell lines. There was no significant difference in $p75^{NTR}$ expression among these breast cancer cell lines (Figure 1a). As TrkA, TrkB and TrkC are high-affinity receptors for NGF, BDNF and NT-3, respectively, the expression patterns of the NTs and TRKs correlate well in these metastatic breast cancer cell lines and the published literature.[30]

Besides increased NT-3 transcript and protein expression, we detected increased secretion of NT-3 in the media from the brain selective breast cancer cell lines compared with the non-brain selective breast cancer cell lines. Using the dot blot analysis, we detected a twofold increased secretion of NT-3 in the conditioned media from the brain selective BCM2 BrainG2 cell line and over threefold increased secretion of NT-3 in the conditioned media from the brain selective MDA-MB 361 cell line compared with the non-brain selective breast cancer cell lines (Figure 1b). Furthermore, we showed that NT-3 elicited significant growth response in the brain selective breast cancer cell lines in the absence of the fetal calf serum but not in the non-brain selective breast cancer cell lines (Figure 1c). In the growth assay, NT concentrations were chosen based on the biological activity specified by the manufacture. Therefore, we confirmed the novel finding that NT-3 expression and secretion are upregulated specifically in the brain selective breast cancer cell lines and showed that NT-3 selectively induces the proliferation of these cells.

NT-3 is expressed in brain metastases from breast cancer patients To further investigate if NT-3 is a potential molecular target for breast cancer brain metastasis, we examined the expression of NT-3 in clinical specimens of brain metastasis originated from breast cancer patients. We performed immunohistochemistry on a cohort of six resected brain metastases of breast cancer and unmatched breast tumors. Representative images of negative control (Figure 2a), NT-3 staining (Figure 2b) and the hematoxylin and eosin staining of a selected brain metastatic lesion from Figure 2b are shown (Figure 2c). Intracellular NT-3 staining was detected in most of the brain metastatic lesions (Figure 2d). All six brain metastases showed high level of NT-3 staining whereas virtually no specific NT-3 staining was seen in the breast tumors (Figure 2e). As expected, NT-3 staining was also not detected in the adult brain tissues (Figure 2f).

NT-3 is necessary for the proliferation of brain selective breast cancer cells in the brain

Brain metastasis of breast cancer has a long latency after the resection of primary breast tumors.[2] Therefore, targeting factors promoting the proliferation of breast cancer cells in the brain will have the highest impact on the survival of patients presented with brain metastases. To monitor the growth of breast cancer cells in the brain without the complication of other metastases, we implanted breast cancer cells in the brain parenchyma at low numbers and showed that the normal parenchyma permits the growth of brain selective breast cancer cell lines but suppress the growth of non-brain selective breast cancer cell lines (Supplementary Figure 1).

To determine if NT-3 is necessary for the growth of brain selective breast cancer cells in the brain, we transfected the brain selective breast cancer cell line, MDA-MB 361, which expresses the highest endogenous NT-3 (Parent), with a short hairpin RNA (shNT-3) against NT-3 or a scramble short hairpin RNA (shRNA control) and examined the growth of four NT-3 knockdown clones in the brain. All four shNT-3 clones showed at least 50% reduction at the mRNA level as determined by quantitative reverse transcription–PCR (qRT–PCR) analysis (Figure 3a) and a similar level of reduction in NT-3 secretion relative to the control cells as determined by the dot blot analysis (Figure 3b). The shRNA constructs used to knock down NT-3 are specific as they did not seem to affect the expression of other NGF family members or TRKs (Supplementary Figure 2A). The first noticeable change we observed in brain selective breast cancer cells with reduced NT-3 expression (shNT-3) was that these cells showed significantly increased cell proliferation compared with the untransfected (Parent) and scrambled shRNA transfected (shRNA Control) MDA-MB 361 cells (Figure 3c).

Next, we examined the effect of NT-3 expression on the growth of brain selective breast cancer cells *in vivo* by implanting 1×10^5 cells from the parent, shRNA control or shNT-3 clones intracranially in the brains of NOD/SCID (nonobese diabetic/severe combined immunodeficient) mice. At day 14 after tumor implantation, we found that the tumor sizes were dramatically reduced in mice injected with shNT-3 clones (>10-fold decrease) than in mice injected with the parent and shRNA control (Figure 3d). Therefore, despite the increased proliferation rate of these cells *in vitro*, they are unable to establish significant tumors in an *in vivo* setting, suggesting that cell growth and other properties of cancer cells may be regulated by environmental clues.

Overexpression of NT-3 increases the metastatic growth of brain selective breast cancer cells *in vivo*

To determine whether an increase in NT-3 expression is sufficient to promote the growth of breast cancer cells in the brain, we transfected NT-3 complementary DNA (cDNA) in the non-brain selective breast cancer cell line, MDA-MB 231. MDA-MB 231 cells with ectopic expression of NT-3 showed at least 10-fold increase of NT-3 at the mRNA level as determined by the qRT–PCR analysis (Figure 4a), and increased secretion of NT-3 compared with the control cells as determined by the dot blot analysis (Figure 4b). Ectopic NT-3 expression in MDA-MB 231 cells appeared to result in a slight increase in TrkC but did not seem to affect the expression of other NGF family members or TRKs

(Supplementary Figure 2B). Interestingly, ectopic expression of NT-3 in MDA-MB 231 cells resulted in a significant decrease in cell proliferation *in vitro* compared with untransfected parent cells (Parent) and empty vector transfected parent cells (Vector Control) (Figure 4c). The effect of NT-3 on cell proliferation *in vitro* is consistent with the shNT3 knockdown clones of brain selective breast cancer cells.

Next, we examined the effect of increased NT-3 expression on the metastatic growth of non-brain selective MDA-MB 231 breast cancer cells *in vivo* by implanting 1×10^5 cells from the WT, Vector Control or NT-3 cDNA-expressing cells intracranially in the brains of NOD/SCID mice. At day 14 after tumor implantation, we found that the tumor sizes were significantly larger in mice injected with NT-3-overexpressing MDA-MB 231 cells (NT-3 cDNA) compared with mice injected with the untransfected (Parent) and empty vector transfected (Vector Control) MDA-MB 231 cells (Figure 4d). Metastatic tumors formed by the NT-3-overexpressing MDA-MB 231 cells showed at least a sixfold increase in tumor volume compared with metastatic tumors formed by the parent and vector control cells (Figure 5d). Together with NT-3 knockdown results, our data indicate that NT-3 is necessary and sufficient to promote the growth of breast cancer cells in the brain microenvironment.

NT-3 is necessary for the early proliferation of metastatic breast cancer cells in the brain microenvironment

So far, we have demonstrated that the selective growth advantage of metastatic breast cancer cells in the brain microenvironment is not mirrored by rapid proliferation *in vitro*. Hence, it is likely that the brain microenvironment exerts a selective pressure on metastatic breast cancer cells *in vivo*. To study the growth of metastatic breast cancer cells with high or low NT-3 in the brain at the early stage of colonization, we employed organotypic brain slice cultures to generate co-cultures of breast cancer cells and brain parenchyma and monitor the co-cultures live for up to a week. The organotypic culture of brain tissues has been successfully used to investigate growth and invasion of glioma cells.[31–33] It has been shown that brain slices can be maintained in culture for a relatively long period of time with intact tissue architecture and preserved biochemical and electrophysiological properties of neuronal cells.

Similar to the *in vivo* xenograft studies, the organotypic brain slice cultures also showed selective preference to permit the growth of breast cancer cells with high NT-3 expression and suppress the growth of breast cancer cells with low NT-3 expression (Figure 5). Hippocampal brain slices were prepared from 8-day-old C57BL mouse pups and placed in individual 24-well tissue culture inserts according to previously published reports[31,32] (see Materials and methods section for details). Green fluorescent protein (GFP)-expressing breast cancer cells with high NT-3 expression (MDA-MB 361, shRNA Control and NT3 cDNA) or low NT-3 expression (MDA-MB 231, Vector Control and shNT-3) were seeded on top of a brain slice and an inverted confocal laser-scanning microscope was used to image GFP colonies formed by the breast cancer cells. Six brain slices were used for quantifying the GFP colonies from each cell line. The total volume of GFP colonies per brain slice were measured using the NIH ImageJ software (U. S. National Institutes of

Health, Bethesda, MD, USA) (area × fluorescent intensity × number of *z*-sections), and an averaged colony volume for each cell line was calculated. Results from three independent experiments were used to derive s.d. After 24 h, we noted that all cells began to migrate into the brain slices, and there was no significant difference in their ability to survive in the organotypic brain slice cultures after 24 h (Figure 5a). However, GFP colonies from brain selective MDA-MB 361 and control shRNA transfected cells started to increase in volume starting from day 3, whereas all four shNT-3 clones showed no significant increase in colony volume over a period of 7 days (Figure 5b). On the contrary, GFP colonies from brain selective MDA-MB 231 and empty vector transfected cells (Vector Control) showed an initial increase in growth in day 3 and progressively decreased in growth over a period of 7 days, whereas NT3-overexpressing MDA-MB 231 cells (NT3 cDNA) showed progressive increase in colony volume from days 3 to 7 (Figure 5b). Together, our data showed that NT-3 expression is critical in sustaining the progressive growth of metastatic breast cancer cells in the brain, although low NT-3 expression did not appear to restrict the proliferation of non-brain selective breast cancer cells early on. Furthermore, we demonstrated that results obtained from organotypic brain slice cultures mimic the growth pattern of metastatic tumors in the *in vivo* xenograft studies, supporting the utility of the organotypic brain slice cultures to study the early events of breast cancer brain metastasis.

NT-3 promotes MET in metastatic breast cancer cells

To gain mechanistic insights on the role of NT-3 in promoting the growth of metastatic breast cancer cells in the brain, we focused on changes induced by overexpressing NT-3 in non-brain selective MDA-MB 231 cells that might acquire the growth advantage in the brain. As we noted earlier, ectopic expression of NT-3 in non-brain selective MDA-MB 231 cells resulted in a decrease in proliferation *in vitro* compared with the untransfected parent and empty vector transfected control cells (Figure 4c). Furthermore, MDA-MB 231 cells with increased NT-3 secretion resembled brain selective breast cancer cells morphologically with increased cell size and cell–cell contact compared with the ameboid-like and migratory morphology of the MDA-MB 231 cells, which exhibit EMT-like phenotype. Therefore, we speculated that NT-3-overexpressing MDA-MB 231 cells underwent MET to gain growth advantages in the brain. To test the hypothesis, we analyzed the expression profiles of myoepithelial (EMT phenotype) and luminal epithelial (MET phenotype) markers in brain selective MDA-MB 361 cells, shRNA knockdown clones of MDA-MB 361 cells (NT-3shRNA), non-brain selective MDA-MB 231 cells and NT-3-overexpressing MDA-MB 231 cells (NT-3 cDNA). We found that MDA-MB 231 cells with increased NT-3 secretion showed increased expression of luminal epithelial genes (*HER2*, *K8/18* and *CD24*) and reduced expression of myoepithelial genes (*EGFR* and *ITGB1*) compared with the parental MDA-MB 231 cells (Figure 6a). In contrast, we detected only significant reduction of the HER2 transcript in the brain selective MDA-MB 361 cells with reduced NT-3 expression compared with the parental MDA-MB 361 cells (Figure 6a). Then, we assessed the protein expression of HER2 and K8/18 proteins in the NT-3 knockdown or overexpressing cells compared with the parental cell lines. In MDA-MB 361 cells, the levels of HER2 were high at the membrane and cell–cell junction (Figure 6b). In NT-3 knockdown MDA-MB 361 cells (MDA-MB 361 + NT-3 shRNA), the cell–cell junction was disorganized and the expression of HER2 expression was low (Figure 6b). On the contrary,

MDA-MB 231 cells had very low level of HER2, whereas NT-3-overexpressing MDA-MB 231 cells (MDA-MB 231 + NT-3 cDNA) had significantly higher level of HER2 at the membrane and cell–cell junction that were similar to MDA-MB 361 cells (Figure 6b). Similar trend was observed for K8/18 protein despite finding no significant change of K8/K18 at the transcriptional level (Figures 6a and b).

In addition to the luminal and myoepithelial markers, we also examined phenotypic changes indicative of MET. Brain selective MDA-MB 361 cells have the typical MET morphology with high level of E-cadherin at the cell membrane (preferred cell–cell contact) and low level of an EMT transcription factor, SNAIL, in the nucleus (Figure 6c, first panel from the left). Non-brain selective MDA-MB 231 cells exhibited the typical EMT morphology expressing very low level of E-cadherin (loss of cell–cell contact) and high level of SNAIL in the nucleus (Figure 6c, third panel from the left). With reduced NT-3 expression, NT-3 knockdown MDA-MB 361 cells showed reduced E-cadherin expression and increased SNAIL expression in the nucleus, which resembled the EMT morphology (Figure 6c, second panel from the left). On the contrary, NT-3-overexpressing MDA-MB 231 cells showed a dramatic increase of E-cadherin at the cell junctions and a dramatic reduction of SNAIL in the nucleus, which resembled the MET morphology (Figure 6c, first panel from the right). As the morphological distinction between EMT and MET cells often results in differences in their migratory ability, we further examined the migratory ability of brain selective and non-brain selective breast cancer cells using an *in vitro* wound-healing assay.[34,35] All cells were seeded at equal density and a wound of an equal width was created in the middle of each well. After 8 h, very few MDA-MB 361 cells (MET phenotype) migrated toward the center of the wound (~90% unfilled gap) compared with the MDA-MB 231 cells (EMT phenotype), which migrated quickly to fill the center of the wound (~20% unfilled gap). (Figure 6d) With reduced NT-3 expression, NT-3 knockdown MDA-MB 361 cells showed increased migratory ability to close the wound (~60% unfilled gap), whereas NT-3-overexpressing MDA-MB 231 cells showed significantly reduced ability to migrate compared with the parental MDA-MB 231 cells (~90% unfilled gap; Figure 6d).

Cancer cells capable of forming macrometastasis in human patients have to disseminate from the primary tumor, survive in circulation, intravasate into the distant tissues and adapt into the foreign microenvironment. By exposing mesenchymal-like MDA-MB 231 cells to cycles of hypoxia and reoxygenation, we isolated a stem-like sub-population that is capable of forming clinically overt distant metastases in the spontaneous tumor xenograft model.[36] To investigate whether the re-epithelialization of metastatic cancer cells we observed in the intracranial brain implantation model also occurs in the spontaneous brain metastasis model, we injected this stem-like sub-population from MDA-MB 231 in the mammary fat pads of female NOD/SCID mice and monitored for spontaneous brain metastasis from these mice. After resecting the primary tumors, three out of six mice developed spontaneous brain metastases. Disruption of the blood–brain barrier by brain metastases was visible for all three mice resembling brain metastasis observed in patients diagnosed with triple-negative or basal-type breast cancer[37] (gross image in Figure 6e left panel; confocal image of brain metastasis GFP colonies from a brain section in Figure 6e right panel). Furthermore, lesions from the spontaneous brain metastasis also showed positive staining of NT-3 and E-

Cadherin (Figure 6f), which support the validity of our observations in the intracranial brain implantation model. Together, we present supporting evidence that increased NT-3 expression is accompanied by re-expressing of E-cadherin during MET in breast cancer cells. Such expression could contribute to the growth advantage of metastatic breast cancer cells in the brain.

NT-3 can cooperate with HER2 to signal growth of brain selective breast cancer cells *in vivo*

We found that in promoting MET in breast cancer cells, NT-3 expression promoted the upregulation of HER2 transcript and proteins as well as the recruitment of HER2 to the cell membrane. We reasoned that HER2 could be activated by NT-3 to transduce growth signal of brain selective breast cancer cells *in vivo* and have found several lines of evidence to support this idea. First, manipulation of NT-3 expression resulted in co-regulation of HER2 protein expression but not TrkC (high-affinity TKR for NT-3; Figure 7a). High level of NT-3 and HER2 was also detected in the metastatic brain lesions derived from both brain selective breast cancer cell lines (Supplementary Figure 3). Second, we found that exogenous NT-3 could stimulate the phosphorylation of HER2 in brain selective MDA-MB 361 cells (top three lanes) and NT-3-overexpressing MDA-MB 231 cells (MDA-MB 231 + NT-3 cDNA; bottom three lanes) (Figure 7b). Furthermore, inhibitors of HER2 signaling, AG879 and Lapatinib, significantly reduced HER2 phosphorylation in the presence of exogenous NT-3 (Figure 7b).

We also determined the sensitivity of metastatic breast cancer cells to these two HER2 inhibitors using dose-response curves and found that brain selective breast cancer cells (MDA-MB 361 and MDA-MB 231 + NT-3 cDNA) were more sensitive to Lapatinib and AG-879 (more cytotoxic) than non-brain selective breast cancer cells (MDA-MB 231 and MDA-MB 361 + shNT-3) (Figure 7c). For example, MDA-MB 361 (half-maximal inhibitory concentration (IC_{50}) = 6.12 μM) and MDA-MB 231 + NT-3 cDNA cells (IC_{50} = 0.68 μM) were 8- or 78-fold, respectively, more sensitive to Lapatinib than MDA-MB 231 cells (IC_{50} = 53.16 μM; Figure 7c). Similarly, knockdown of NT-3 in MDA-MB 361 cells (MDA-MB 361 + NT-3 shRNA) rendered the MDA-MB 361 cells much less sensitive to Lapatinib (IC_{50} = 51.3 μM) and AG-879 (IC_{50} = 43.7 μM; Figure 7c). To further demonstrate that HER2 can transduce growth signaling in brain selective breast cancer cells *in vivo*, we implanted brain metastatic breast cancer cells (MDA-MB 361 and MDA-MD 231 + NT3 cDNA) intracranically and treated the tumors with either Lapatinib or AG-879 at 3 days after the tumor cell injection. Then, 20 μM of Lapatinib, AG-879 or 0.1% dimethylsulfoxide in saline were infused intracranially via a mini-osmotic pump that delivers compounds at a rate of 0.25 μl per hour. At 7 days after the drug treatment, mice were killed and the metastatic tumor volume in the brain was quantified. During the treatment period, we did not observe any obvious toxicity of the treated mice. After the HER2-targeted treatments, we found a dramatic reduction of metastatic tumors in mice treated with AG-879 or Lapatinib compared with those treated with the dimethylsulfoxide control (Figure 7d). Together, we concluded that NT-3 could induce HER2 signaling to promote the metastatic growth of breast cancer cells *in vivo* and render the metastatic tumors sensitive to HER2 inhibition.

NT-3 reduces the activation of microglia to evade the CNS immune response

Thus far, our results showed that breast cancer cells capable of generating brain metastasis have opposite characteristics from metastatic breast cancer cells from the primary tumor. Our data further demonstrated the selectivity of the brain microenviron-ment. Therefore, we speculated that NT-3 promotes MET of breast cancer cells to elicit protective host response. The CNS has evolved as an immune-privileged site to protect its vital functions from damaging immune-mediated inflammation. A CNS-adapted system of surveillance continuously evaluates local changes in the nervous system and communicates to the peripheral immune system during an injury or a disease. It has been reported that reactive glia are recruited by highly proliferative brain metastases of breast cancer.[27] One type of the glia cells in the CNS, microglia, plays an important function in the immune response in the CNS. Microglia scavenge the CNS for damaged neurons, plaques and infectious agents. They are capable of recognizing foreign bodies, phagocytosing them and acting as antigen-presenting cells. Last, microglia are extremely sensitive to even small pathological changes in the CNS.[38]

Microglia secrete a variety of factors in response to environmental changes, which enables them to be cytotoxic or cytoprotective when stimulated by different effectors. It has been shown that microglia can secrete NTs, including NT-3, and NT-3 has an inhibitory effect on the activation of microglia, and although microglial activation is stimulated by bacterial lipopolysaccharide, preincubation with NT-3 can inhibit this lipopolysaccharide-mediated activation.[28] To visualize the response of microglia to the presence of metastatic breast cancer cells in the CNS parenchyma, we used immunofluorescence against Iba-1 (ionized calcium binding adaptor molecule 1). Iba-1 is a 17-kDa EF hand protein expressed in macrophages/microglia that is upregulated during the activation of these cells.[39] Using scanning confocal microscopy, we quantified the number of Iba-1-positive microglia surrounding and infiltrating the metastatic tumors based on pixel intensity as well as cell morphological changes. Activated microglia were defined as cells with a cell body >10 μm in diameter, <2 short, thick processes and intense Iba-1 immunoreactivity. We counted cell numbers at three different time points.

Based on Iba-1 staining, we found that microglia were recruited to the metastatic tumors derived from the non-brain selective MDA-MB 231 breast cancer cells as early as day 1 and increased dramatically at day 3 (Figure 8a, bottom panel). On the contrary, significantly less microglia were recruited to the metastatic tumors derived from the brain-derived MDA-MB 361 breast cancer cells (Figure 8a, top panel). Magnified images showed activated microglia in the metastatic lesions (Figure 8a, ×100). We calculated the numbers of activated microglia surrounding and infiltrating the metastatic lesions and found persistently higher percentage of activated microglia in the metastatic tumors derived from the non-brain selective MDA-MB 231 and MDA-MB 361 + shNT-3 breast cancer cells than the tumors derived from brain selective MDA-MB 361 and MDA-MB 231 + NT-3 cDNA breast cancer cells. Furthermore, increased activation of microglia correlated negatively with the metastatic growth of breast cancer cells *in vivo* (Figure 8b). Interestingly, the growth trend of brain and non-brain selective breast cancer cells *in vivo* resembled closely the growth trend of these cells on organotypic brain slice cultures. For non-brain selective breast cancer

cells, there was an initial increase in growth at the early time point (day 3) and progressively decreased at the later time points. As MDA-MB 361 + shNT-3 breast cancer cells only showed a partial conversion from the epithelial-like phenotype to EMT-like phenotype, these cells did not proliferate as fast as the EMT-like MDA-MB 231 cells at the early time point (Figure 8b) and similar growth trend was observed in the organotypic culture assay as well (Figure 5b). On the contrary, brain selective breast cancer cells grow slow but steadily over the measured period to form macrometastasis. Therefore, we believe that the kinetic of tumor growth in the *ex vivo* and *in vivo* brain parenchyma is influenced by the interaction of tumor cells and microglia. Together, our data suggest that NT-3 reduced the activation of microglia recruited to the metastatic tumors and allowed for a 'permissive' microenvironment to promote the metastatic growth of breast cancer cells.

DISCUSSION

Metastasis accounts for the majority of cancer-related deaths in the United States. Breast cancer metastases are often found in the bone, lung, brain and liver.[5] Breast cancer brain metastasis is the main source of metastatic brain disease in women,[40] and has a high mortality rate as a result of resistance to chemotherapies[2] and a low success rate of radiotherapy.[41]

Ample evidence supports the idea that transformation of cancer cells similar to EMT allows them to gain invasive and metastatic abilities and separate from the primary tumor.[42,43] After undergoing EMT, these cancer cells gain access to distant sites through hematogenous or lymphatic routes of dissemination and then can extravasate into secondary tissues to establish micrometastases. It has also become clear that extrinsic barriers imposed by the microenvironment at secondary sites rather than the systemic spread can be the rate-limiting step of metastatic progression.[44–48] In this study, we showed that increased expression of a growth factor, NT-3, in metastatic breast cancer cells allows them to overcome intrinsic and extrinsic barriers in the brain microenvironment. Furthermore, our data support the concept that EMT is reversible at the metastatic sites. We showed that decreasing NT-3 expression in brain selective breast cancer cells resulted in a partial conversion of the epithelial phenotype to the EMT phenotype and significant reduced metastatic growth of these cells in the brain. Conversely, ectopic expression of NT-3 in non-brain selective breast cancer cells resulted in a reversion from the EMT-like phenotype to the epithelial-like phenotype, particularly with respect to morphology and functional suppression of migration and proliferation, and resulted in significantly increased metastatic growth of these cells in the brain. In addition to the induction of phenotypic conversions, we also found a previously unknown link between NT-3 and HER2 signaling in the brain metastatic cells. We showed that NT-3 can promote the growth of metastatic breast cancer cells in the brain parenchyma through HER2, and that blocking HER2 signaling significantly reduces the metastatic growth of these cells in the brain. HER2 overexpression in primary breast tumors has been associated with dismal prognosis and high incidence of brain metastasis.[49,50] Multicenter clinical trials have been conducted to investigate the preventive and antitumor benefit of Lapatinib (HER2 inhibitor) in patients with HER2-positive breast cancer and progressive brain metastasis.[51–53] Overall, Lapatinib seems to have the highest impact on volumetric changes of brain metastasis. Furthermore, overexpressing HER2 in a HER2-negative brain metastatic breast cancer cell

line, 231-BR, did not affect the number of micrometastases in the brain but yielded increased numbers of large metastases instead.[54] Together, we believe that HER2 signaling is important in promoting the growth of metastatic breast cancer cells and not the colonizing ability of these cells. Furthermore, HER2 can be reactivated by intrinsic factors in the metastatic breast cancer cells to promote the metastatic growth and therefore can be targeted for reducing tumor volume in breast cancer patients.

Microenvironment plays an important role in the survival and growth of tumor cells at the metastatic sites. However, little is known about the interactions between the brain parenchyma and tumor cells. In this paper, we explored the interaction between microglia and metastatic breast cancer cells, but more importantly the response of microglia to intrinsic characteristics of metastatic breast cancer cells. We showed that the epithelial phenotype correlates with less microglia activation and favors the growth of breast cancer cells in the brain parenchyma. We found that brain selective metastatic breast cancer cells with the MET-like phenotype were surrounded by less activated microglia in the brain parenchyma; however, knocking down NT-3 in these cells made them exhibit an EMT-like phenotype; it also resulted in increased numbers of activated microglia surrounding the metastatic cells. Similarly, non-brain selective breast cancer cells with the EMT-like phenotype were surrounded by more activated microglia in the brain parenchyma, and overexpressing NT-3 in these cells made them exhibiting more epithelial phenotype and reducing the number of activated microglia in the surrounding. In human patients, the presence of glia cells, including microglia in breast brain metastases, has been reported, and these CNS immune cells have been implicated in promoting tumor colonization.[27] Therefore, manipulating the cytoprotective or cytotoxic response of the CNS-resident immune cells might provide a new therapeutic avenue to interfere with the tumor growth in the brain.

MATERIALS AND METHODS

Cell lines and tissue culture

MDA-MB 231 was purchased from American Type Culture Collection (ATCC, Manassas, VA, USA). BCM2 breast cancer cell line was obtained from Dr Felding-Harbermann's laboratory (The Scripps Research Institute, La Jolla, CA, USA). BCM2 BrainG2 cells are brain-derived cells from injecting BCM2 breast cancer cells intravenously.[13] MDA-MB 231, BCM2 and BCM2 BrainG2 breast cancer cells were cultured in minimum essential medium (Life Technologies Corporation, Carlsbad, CA, USA) supplemented with 10% fetal bovine serum (Hyclone, ThermoFisher, Waltham, MA, USA), 2 mM L-glutamine, 1 mM sodium pyruvate, 1 mM non-essential amino acids and 1% vitamin (Hyclone). MDA-MB 361 cells were cultured in L15 medium (Corning Incorporated, Corning, NY, USA) supplemented with 20% fetal bovine serum. All cell cultures except MDA-MB 361 cells were maintained at 37 °C and in 5% CO_2. MDA-MB 361 cells were maintained at 37 °C and in 0% CO_2. Cells in monolayer cultures were propagated in tissue culture-treated flasks.

A collection of lentiviruses carrying six different short hairpin sequences against NT-3 gene was purchased and used to generate the NT-3 knockdown cell lines (The MISSION shRNA collection, Sigma Aldrich, St Louis, MA, USA). A short-hairpin sequence from the NT-3

shRNA collection that did not result in NT-3 knockdown was used as the shRNA control. Cells were infected first with the Lenti-GFP lentiviral particles (Lentigen, Baltimore, MD, USA) and then infected with shNT-3 lentivirus (multiplicity of infection of 10). A total of 1 μg/ml of puromycin was used to generate stable cell lines. The NT-3-overexpression cells were made from the NT3 cDNA gene inserted into the GIPZ Lentiviral vector obtained from Open Biosystems (Huntsville, AL, USA). Cells were transfected with either an empty vector or NT-3 cDNA vector using Lipofectamine 2000 (Invitrogen, Carlsbad, CA, USA) and selected with 250 μg/ml of G418. Consistent intensity of GFP expression among all cell lines was verified using flow cytometry.

Analysis of the mRNA expression by qRT–PCR assay

Total RNA was isolated from each cell line using RNA Extraction Kit (Qiagen, Valencia, CA, USA) according to the manufacturer's instructions. Total RNA (2 μg) from each cell line was reverse transcribed using random primers and the High Capacity cDNA synthesis Kit (Life Technologies Corporation). The resulting cDNAs were mixed with the SYBR PCR master mix (Applied Biosystems) and run on the StepOnePlus Applied Biosystems Real-time PCR machine. One cycle of denaturing step (10 min at 95 °C) was applied, followed by 35 cycles of amplification (15 s at 95 °C and 1 min at 58 °C), with fluorescence measured during the extension. Primers used in this study are listed below.

GAPDH: 5′-CAAGCTCATTTCCTGGTATGAC-3′(forward)

5′-CAGTGAGGGTCTCTCTCTTCCT-3′(reverse)

NT-3: 5′-TACGCGGAGCATAAGAGTCA-3′(forward)

5′-CCAGCCCACGAGTTTATTGT-3′(reverse)

NGF: 5′-CCAAGGACGCAGCTTTCTAT-3′(forward)

5′-CTCCGGTGAGTCCTGTTGAA-3′(reverse)

BDNF: 5′-AGCGTGAATGGGCCCAAGGCA-3′(forward)

5′-TGTGCCGTCCCGCCCGACA-3′(reverse)

NT-4/5: 5′-GACAGGAGGCACTGGGTATC-3′(forward)

5′-CCTGAGGTCTCTCAGCATCC-3′(reverse)

5′-TGTGCCGTCCCGCCCGACA-3′(reverse)

TrkA: 5′-CCATCGTGAAGAGTGGTCTCC-3′(forward)

5′-GGTGACATTGGCCAGGGTCA-3′(reverse)

TrkC: 5′-AGCACTGCATCGAGTTTGTG-3′(forward)

5′-AGTGGGTTTTTGGCAATGAG-3′(reverse)

$p75^{NTR}$: 5′-TGAGTGCTGCAAAGCCTGCAA-3′(forward)

5′-TCTCATCCTGGTAGTAGCCGT-3′(reverse)

The relative quantification value reflects the fold changes of mRNA expression in each cell line compared with the parental cell line (MDA-MB 231). It was calculated using the comparative C_T ($\Delta\Delta C_T$) method and Step-OnePlus software v2.0.1 (Applied Biosystems) and normalized by the expression of the house keeping gene, *GAPDH*. Three independent experiments were performed to derive average relative quantification and s.d.

Dot blot analysis

Conditioned media were prepared from cell lines grown in serum free media for 3 days. Conditioned media were collected and concentrated using Amicon Ultra-4 Centrifugal Filter Unit (Millipore, Billerica, MA, USA). Protein (10 μg) was spotted onto a nitrocellulose membrane using a Bio-Dot microfiltration apparatus (Bio-Rad, Hercules, CA, USA), and equal loading of proteins was visualized by Ponceau S staining. Immunoassay was performed according to the standard procedures using an antibody against NT-3 (1:200; R&D Systems, Minneapolis, MN, USA). Secondary antibodies conjugated with either AF680 (Invitrogen) or CW800 (LICOR Biosciences, Lincoln, NE, USA) were used to visual protein bands using the Odyssey Infrared Imager (LICOR Biosciences). The intensity of each spot was quantified using the NIH ImageJ software. Triplicate sets were used to derive s.d.. Non-brain selective cells were used as the reference cell lines to calculate the relative fold difference of secreted NT-3.

Cell proliferation assay with recombinant NT-3

Cells were seeded into a 96-well tissue culture plate at a density of 3×10^4 cells/well and allowed to recover in complete medium overnight. The next day, cells were washed 3 times with phosphate-buffered saline (PBS) and treated with serum-free media (control), serum-free media and various amount of purified recombinant NT-3 (Cell Sciences, Canton, MA, USA) based on the suggested bioactivity of each growth factor by the manufacture. After 24 h, cell growth was measured using the CCK-8 assay (Dojindo Molecular Technologies, Inc., Rockville, MD, USA). The CCK-8 assay measures the reduction of a tetrazolium salt, WST-8, to a formazan dye by live cells. Reduction of WST-8 is an indirect measurement of the number of live cells based on their metabolic activity. The percentage of increase in cell numbers was derived from comparing the absorbance of 450 nm of treated wells with the control wells.

Immunohistochemistry of tissue sections and immunostaining of cells

Frozen sections of brain metastases from patients with primary breast cancer were obtained from The Brain Tumour Tissue Bank, London Health Sciences Centre (Ontario, Canada). Immunostaining was performed according to standard procedures using an antibody against NT-3 (1:50; R&D Systems) and visualized using a chromogenic substrate, DAB, and hematoxylin for counterstaining. An isotype-matched control was included as negative control. For staining the 4% paraformaldehyde perfused brains containing metastatic lesions from intracranial injection of metastatic breast cancer cells, the brains were first sectioned coronally and blocked with 2% bovine serum albumin in PBS-T (PBS/0.1% Triton X-100). Then, sections were incubated with rabbit anti-Iba-1 (Wako, Richmond, VA, USA), mouse anti-NT-3 (Origene, Rockville, MD, USA) or rabbit anti-HER2 (Cell Signaling, Danvers,

MA, USA) antibodies. Secondary antibodies, Alexa Fluor 555 (Invitrogen), anti-rabbit and Cy5 anti-mouse (Jackson ImmunoResearch, West Groove, PA, USA), were used for visualization by the scanning confocal microscope. Nuclei were visualized using 4′,6-diamidino-2-phenylindole (Invitrogen). For immunocytochemistry, cells were seeded in Lab-Tek chamber slides (Thermo Nalge Nunc, Waltham, MA, USA) and grown until ~80% confluence as a monolayer. Then, cells in the chamber slides were washed with PBS, and fixed with 4% paraformaldehyde at 37 °C for 10 min. After fixing the cells, cells were washed with PBS, blocked with 2% bovine serum albumin in PBS-T and incubated with anti-HER2, anti-K8/18 (Abcam, Cambridge, MA, USA), E-cadherin (Abcam) or Snail (Cell Signaling). Alexa Fluor 555 secondary antibody (Invitrogen) was used for visualization by the scanning confocal microscope. Nuclei were visualized using 4′,6-diamidino-2-phenylindole (Invitrogen).

Intracranial injection and imaging of metastatic breast cancer cells

All animal procedures were approved by the Stony Brook University Institutional Animal Care and Use Committee. The 4–6-week-old female NOD/SCID mice (Harlan Laboratories, Inc., Indianapolis, IN, USA) were anesthetized with 2.5% avertin. A midline incision was made on the scalp and a small hole was drilled onto the skull at bregma, 1 mm anteroposterior and + 1.8 mm mediolateral. A 2.5 μl Hamilton syringe with a 22-gauge needle was used to inject 1×10^5 GFP-expressing human breast cancer cells in 2.5 μl into the brain at the depth of 1.5 mm.

Brains were harvested at various time points to analyze the metastatic tumor lesions after the initial tumor injection. To harvest the brains, mice were anesthetized with 2.5% avertin and transcardially perfused with 50 ml of PBS, followed by 50 ml of 4% paraformaldehyde. Brains were then removed and postfixed in 4% paraformaldehyde overnight at 4 °C, followed by 30% sucrose cryoprotection overnight at room temperature.

Coronal brain sections of 1 mm thicknesses were made from each mouse, and GFP metastatic tumor lesions from each section were imaged using the scanning laser confocal microscope (LSM 510 Zeiss, Thornwood, NY, USA). For each brain slice, serial sections were made every 2 μm downward from the basal plane (surface of the brain slice, 0 μm) to the bottom of the slice to image the metastatic breast cancer cells at the different depth. Images of *z*-sections were then used to calculate the tumor volume (mm^3) using the NIH ImageJ Software. The sum of all *z*-sections was used as the tumor volume for each brain.

Organotypic brain slice cultures

Organotypic brain slice cultures were prepared as described previously.[31,32] In brief, brains were harvested from P8-P10 newborn mice and the frontal slice of the caudal cerebrum extracted. The slice was transversally sectioned at a 350-μm thickness on a sliding vibratome. Tissue slices were grown individually in Millicell-CM 0.45 μm cell culture inserts (Millipore) and cultured in 50% minimum essential medium, 25% fetal bovine serum, 25% Hanks' buffered saline solution, 2.64 mg/ml glucose, penicillin and streptomycin at 34 °C and 5% CO_2. Brain sections were cultured for 10 days to allow for stabilization. GFP-expressing cells were then co-cultured on each section at a density of

1000 cells in 1 μl of Hanks' buffered saline solution. Five representative images of each brain slice co-culture were taken over a period of 7 days. Images were taken using the scanning laser confocal microscope (Zeiss LSM 510). For each culture, 35 serial *z*-stacks were taken every 1 μm downward from the basal plane (surface of the brain slice, 0 μm) to the bottom of the tissue. Images of the serial stack were then merged and NIH ImageJ Software was used to quantify the total fluorescent pixel intensity of each GFP colony. A total of six different brain slices were used per cell line per experiment. The sum of pixel intensity from GFP colonies in each brain slice was calculated and compared over time.

Animal and surgery

All animal procedures were performed in accordance with an approved protocol by the Stony Brook University institutional animal care and use committee. NOD/SCID mice were purchased from the Jackson Laboratory (Bar Harbor, ME, USA). Female mice, 4 to 6 weeks old, were used for tumor injections. Human breast cancer cells were suspended in sterile Hanks' buffered salt solution and injected into the third thoracic mammary gland. Tumor formation was assessed by palpation at least once a week. A caliper was used to measure the length and width of tumors at least once a week. A standard formula of calculating tumor volume (mm^3) was used: length × $(width)^2/2$. A minimum of duplicate experiments were performed for each cell number.

Statistical analysis

The Student's *t*-test was used for statistical analysis. A *P*-value of <0.05 was considered statistically significant.

Wound-healing assay

Cells were seeded into a 12-well plate and grown under normal culturing conditions until reaching ~70–80% confluence as a monolayer. A gentle scratch was then made across the center of the well with a sterile pipette tip to create a straight line in one direction. After scratching, the wells were washed with medium to remove the detached cells, and then fresh medium was added to each well. Images were taken at × 20 magnification every 2 h from 0 to 8 h. The gap distance was analyzed by the NIH ImageJ. Minimum three wells per cell line were used to evaluate the gap distance, and three replicate experiments were performed to confirm the results.

Acknowledgments

This work was supported by grants to EIC from the Susan Komen Foundation and the Mary Anita Conroy Memorial Breast Cancer Fund from the Manhasset Women's Coalition Against Breast Cancer. S Tsirka and K Ji were supported by R01NS42168.

References

1. Welch DR, Steeg PS, Rinker-Schaeffer CW. Molecular biology of breast cancer metastasis. Genetic regulation of human breast carcinoma metastasis. Breast Cancer Res. 2000; 2:408–416. [PubMed: 11250734]
2. Weil RJ, Palmieri DC, Bronder JL, Stark AM, Steeg PS. Breast cancer metastasis to the central nervous system. Am J Pathol. 2005; 167:913–920. [PubMed: 16192626]

3. Price JE. Metastasis from human breast cancer cell lines. Breast Cancer Res Treat. 1996; 39:93–102. [PubMed: 8738609]

4. Minn AJ, Gupta GP, Siegel PM, Bos PD, Shu W, Giri DD, et al. Genes that mediate breast cancer metastasis to lung. Nature. 2005; 436:518–524. [PubMed: 16049480]

5. Lu X, Kang Y. Organotropism of breast cancer metastasis. J Mammary Gland Biol Neoplasia. 2007; 12:153–162. [PubMed: 17566854]

6. Ohno S, Ishida M, Kataoka A, Murakami S. Brain metastasis of breast cancer. Breast Cancer. 2004; 11:27–29. [PubMed: 14718788]

7. Kirsch DG, Loeffler JS. Brain metastases in patients with breast cancer: new horizons. Clin Breast Cancer. 2005; 6:115–124. [PubMed: 16001989]

8. Chang EL, Lo S. Diagnosis and management of central nervous system metastases from breast cancer. Oncologist. 2003; 8:398–410. [PubMed: 14530493]

9. Puduvalli VK. Brain metastases: biology and the role of the brain microenvironment. Curr Oncol Rep. 2001; 3:467–475. [PubMed: 11595114]

10. Nathoo N, Chahlavi A, Barnett GH, Toms SA. Pathobiology of brain metastases. J Clin Pathol. 2005; 58:237–242. [PubMed: 15735152]

11. Tomasevic Z, Radosevic-Jelic L, Jovanovic D, Milovanovic Z, Tomasevic ZM, Jelic S, et al. Brain metastases as late breast cancer relapse. Single institution experience and review of the literature. J BUON. 2009; 14:225–228. [PubMed: 19650170]

12. Piccirilli M, Sassun TE, Brogna C, Giangaspero F, Salvati M. Late brain metastases from breast cancer: clinical remarks on 11 patients and review of the literature. Tumori. 2007; 93:150–154. [PubMed: 17557561]

13. Chen EI, Hewel J, Krueger JS, Tiraby C, Weber MR, Kralli A, et al. Adaptation of energy metabolism in breast cancer brain metastases. Cancer Res. 2007; 67:1472–1486. [PubMed: 17308085]

14. Huang EJ, Reichardt LF. Trk receptors: roles in neuronal signal transduction. Annu Rev Biochem. 2003; 72:609–642. [PubMed: 12676795]

15. Adriaenssens E, Vanhecke E, Saule P, Mougel A, Page A, Romon R, et al. Nerve growth factor is a potential therapeutic target in breast cancer. Cancer Res. 2008; 68:346–351. [PubMed: 18199526]

16. Descamps S, Pawlowski V, Revillion F, Hornez L, Hebbar M, Boilly B, et al. Expression of nerve growth factor receptors and their prognostic value in human breast cancer. Cancer Res. 2001; 61:4337–4340. [PubMed: 11389056]

17. Vanhecke E, Adriaenssens E, Verbeke S, Meignan S, Germain E, Berteaux N, et al. Brain-derived neurotrophic factor and neurotrophin-4/5 are expressed in breast cancer and can be targeted to inhibit tumor cell survival. Clin Cancer Res. 2011; 17:1741–1752. [PubMed: 21350004]

18. Hondermarck H. Nerve growth factor: the dark side of the icon. Am J Pathol. 2008; 172:865–867. [PubMed: 18349120]

19. Kowalski PJ, Rubin MA, Kleer CG. E-cadherin expression in primary carcinomas of the breast and its distant metastases. Breast Cancer Res. 2003; 5:R217–R222. [PubMed: 14580257]

20. Chao YL, Shepard CR, Wells A. Breast carcinoma cells re-express E-cadherin during mesenchymal to epithelial reverting transition. Mol Cancer. 2010; 9:179. [PubMed: 20609236]

21. Chaffer CL, Dopheide B, McCulloch DR, Lee AB, Moseley JM, Thompson EW, et al. Upregulated MT1-MMP/TIMP-2 axis in the TSU-Pr1-B1/B2 model of metastatic progression in transitional cell carcinoma of the bladder. Clin Exp Metastasis. 2005; 22:115–125. [PubMed: 16086232]

22. Chaffer CL, Brennan JP, Slavin JL, Blick T, Thompson EW, Williams ED. Mesenchymal-to-epithelial transition facilitates bladder cancer metastasis: role of fibroblast growth factor receptor-2. Cancer Res. 2006; 66:11271–11278. [PubMed: 17145872]

23. Yates CC, Shepard CR, Stolz DB, Wells A. Co-culturing human prostate carcinoma cells with hepatocytes leads to increased expression of E-cadherin. Br J Cancer. 2007; 96:1246–1252. [PubMed: 17406365]

24. Oltean S, Sorg BS, Albrecht T, Bonano VI, Brazas RM, Dewhirst MW, et al. Alternative inclusion of fibroblast growth factor receptor 2 exon IIIc in Dunning prostate tumors reveals unexpected

epithelial mesenchymal plasticity. Proc Natl Acad Sci USA. 2006; 103:14116–14121. [PubMed: 16963563]

25. Vincan E, Darcy PK, Smyth MJ, Thompson EW, Thomas RJ, Phillips WA, et al. Frizzled-7 receptor ectodomain expression in a colon cancer cell line induces morphological change and attenuates tumor growth. Differentiation. 2005; 73:142–153. [PubMed: 15901282]
26. He BP, Wang JJ, Zhang X, Wu Y, Wang M, Bay BH, et al. Differential reactions of microglia to brain metastasis of lung cancer. Mol Med. 2006; 12:161–170. [PubMed: 17088948]
27. Fitzgerald DP, Palmieri D, Hua E, Hargrave E, Herring JM, Qian Y, et al. Reactive glia are recruited by highly proliferative brain metastases of breast cancer and promote tumor cell colonization. Clin Exp Metastasis. 2008; 25:799–810. [PubMed: 18649117]
28. Tzeng SF, Huang HY, Lee TI, Jwo JK. Inhibition of lipopolysaccharide-induced microglial activation by preexposure to neurotrophin-3. J Neurosci Res. 2005; 81:666–676. [PubMed: 16015620]
29. Elkabes S, DiCicco-Bloom EM, Black IB. Brain microglia/macrophages express neurotrophins that selectively regulate microglial proliferation and function. J Neurosci. 1996; 16:2508–2521. [PubMed: 8786427]
30. Tagliabue E, Castiglioni F, Ghirelli C, Modugno M, Asnaghi L, Somenzi G, et al. Nerve growth factor cooperates with p185(HER2) in activating growth of human breast carcinoma cells. J Biol Chem. 2000; 275:5388–5394. [PubMed: 10681513]
31. Matsumura H, Ohnishi T, Kanemura Y, Maruno M, Yoshimine T. Quantitative analysis of glioma cell invasion by confocal laser scanning microscopy in a novel brain slice model. Biochem Biophys Res Commun. 2000; 269:513–520. [PubMed: 10708585]
32. Jung S, Kim HW, Lee JH, Kang SS, Rhu HH, Jeong YI, et al. Brain tumor invasion model system using organotypic brain-slice culture as an alternative to in vivo model. J Cancer Res Clin Oncol. 2002; 128:469–476. [PubMed: 12242510]
33. Cho S, Wood A, Bowlby MR. Brain slices as models for neurodegenerative disease and screening platforms to identify novel therapeutics. Curr Neuropharmacol. 2007; 5:19–33. [PubMed: 18615151]
34. Menon MB, Ronkina N, Schwermann J, Kotlyarov A, Gaestel M. Fluorescence-based quantitative scratch wound healing assay demonstrating the role of MAPKAPK-2/3 in fibroblast migration. Cell Motil Cytoskeleton. 2009; 66:1041–1047. [PubMed: 19743408]
35. Yarrow JC, Perlman ZE, Westwood NJ, Mitchison TJ. A high-throughput cell migration assay using scratch wound healing, a comparison of image-based readout methods. BMC Biotechnol. 2004; 4:21. [PubMed: 15357872]
36. Louie E, Nik S, Chen JS, Schmidt M, Song B, Pacson C, et al. Identification of a stem-like cell population by exposing metastatic breast cancer cell lines to repetitive cycles of hypoxia and reoxygenation. Breast Cancer Res. 2010; 12:R94. [PubMed: 21067584]
37. Yonemori K, Tsuta K, Ono M, Shimizu C, Hirakawa A, Hasegawa T, et al. Disruption of the blood brain barrier by brain metastases of triple-negative and basal-type breast cancer but not HER2/neu-positive breast cancer. Cancer. 2010; 116:302–308. [PubMed: 19937674]
38. Perry VH, Cunningham C, Holmes C. Systemic infections and inflammation affect chronic neurodegeneration. Nat Rev Immunol. 2007; 7:161–167. [PubMed: 17220915]
39. Ohsawa K, Imai Y, Sasaki Y, Kohsaka S. Microglia/macrophage-specific protein Iba1 binds to fimbrin and enhances its actin-bundling activity. J Neurochem. 2004; 88:844–856. [PubMed: 14756805]
40. Klos KJ, O'Neill BP. Brain metastases. Neurologist. 2004; 10:31–46. [PubMed: 14720313]
41. Kwon HC, Oh SY, Kim SH, Lee S, Kwon KA, Choi YJ, et al. Clinical outcomes and breast cancer subtypes in patients with brain metastases. Onkologie. 33:146–152. [PubMed: 20389140]
42. Trimboli AJ, Fukino K, de Bruin A, Wei G, Shen L, Tanner SM, et al. Direct evidence for epithelial-mesenchymal transitions in breast cancer. Cancer Res. 2008; 68:937–945. [PubMed: 18245497]
43. Tse JC, Kalluri R. Mechanisms of metastasis: epithelial-to-mesenchymal transition and contribution of tumor microenvironment. J Cell Biochem. 2007; 101:816–829. [PubMed: 17243120]

44. Montel V, Huang TY, Mose E, Pestonjamasp K, Tarin D. Expression profiling of primary tumors and matched lymphatic and lung metastases in a xenogeneic breast cancer model. Am J Pathol. 2005; 166:1565–1579. [PubMed: 15855655]
45. Husemann Y, Geigl JB, Schubert F, Musiani P, Meyer M, Burghart E, et al. Systemic spread is an early step in breast cancer. Cancer Cell. 2008; 13:58–68. [PubMed: 18167340]
46. Mehlen P, Puisieux A. Metastasis: a question of life or death. Nat Rev Cancer. 2006; 6:449–458. [PubMed: 16723991]
47. Kim JW, Wong CW, Goldsmith JD, Song C, Fu W, Allion MB, et al. Rapid apoptosis in the pulmonary vasculature distinguishes non-metastatic from metastatic melanoma cells. Cancer Lett. 2004; 213:203–212. [PubMed: 15327836]
48. MacDonald IC, Groom AC, Chambers AF. Cancer spread and micrometastasis development: quantitative approaches for in vivo models. Bioessays. 2002; 24:885–893. [PubMed: 12325121]
49. Choi YH, Ahn JH, Kim SB, Jung KH, Gong GY, Kim MJ, et al. Tissue microarray-based study of patients with lymph node-negative breast cancer shows that HER2/neu overexpression is an important predictive marker of poor prognosis. Ann Oncol. 2009; 20:1337–1343. [PubMed: 19221151]
50. Bendell JC, Domchek SM, Burstein HJ, Harris L, Younger J, Kuter I, et al. Central nervous system metastases in women who receive trastuzumab-based therapy for metastatic breast carcinoma. Cancer. 2003; 97:2972–2977. [PubMed: 12784331]
51. Lin NU, Carey LA, Liu MC, Younger J, Come SE, Ewend M, et al. Phase II trial of lapatinib for brain metastases in patients with human epidermal growth factor receptor 2-positive breast cancer. J Clin Oncol. 2008; 26:1993–1999. [PubMed: 18421051]
52. Cameron D, Casey M, Press M, Lindquist D, Pienkowski T, Romieu CG, et al. A phase III randomized comparison of lapatinib plus capecitabine versus capecitabine alone in women with advanced breast cancer that has progressed on trastuzumab: updated efficacy and biomarker analyses. Breast Cancer Res Treat. 2008; 112:533–543. [PubMed: 18188694]
53. Geyer CE, Forster J, Lindquist D, Chan S, Romieu CG, Pienkowski T, et al. Lapatinib plus capecitabine for HER2-positive advanced breast cancer. N Engl J Med. 2006; 355:2733–2743. [PubMed: 17192538]
54. Palmieri D, Bronder JL, Herring JM, Yoneda T, Weil RJ, Stark AM, et al. Her-2 overexpression increases the metastatic outgrowth of breast cancer cells in the brain. Cancer Res. 2007; 67:4190–4198. [PubMed: 17483330]

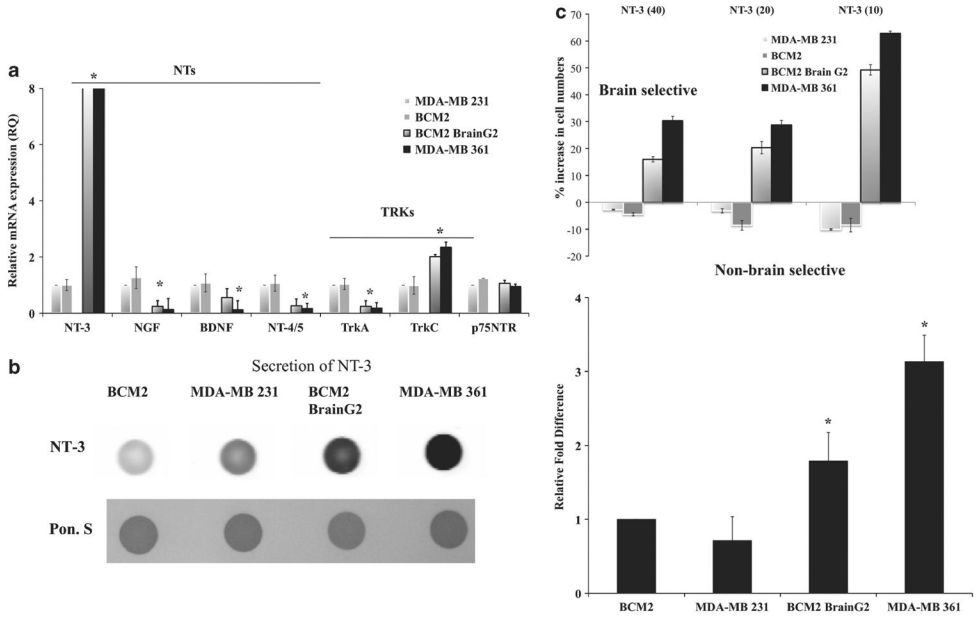

Figure 1.

Expression profiles of NTs and neurotrophin TRKs in brain selective and non-brain selective breast cancer cell lines. (**a**) mRNA expression of NTs and TRKs in brain selective (MDA-MB 361 and BCM2 BrainG2) and non-brain selective (MDA-MB 231 and BCM2) breast cancer cells. Quantitative real-time PCR was used to compare the mRNA levels of these cell lines. MDA-MB 231 was used as the reference cell line to derive relative quantification (RQ) values for mRNA expression. (**b**) Secretion of NT-3 in the conditioned media by the dot blot analysis. A total of 20 μg of proteins from the conditioned media of each cell line were spotted on the nitrocellulose membrane. Antibody against NT-3 was used to detect the presence of secreted NT-3 in the conditioned media. Ponceau S staining was used to show equal loading of proteins from the conditioned media. Triplicate dots per cell line were used for quantitative analysis (see Materials and methods for quantitative analysis). BCM2 NT-3 intensity was used as the reference to derive relative fold difference of secreted NT-3 in other cell lines. (**c**) Growth response elicited by NT-3 in the serum-free culture media. The growth response was measured by the cell proliferation assay. Values in parenthesis are the concentrations of NT-3 used in this assay in ng/ml. *Statistically significant values (P<0.05). A full colour version of this figure is available at the *Oncogene* journal online.

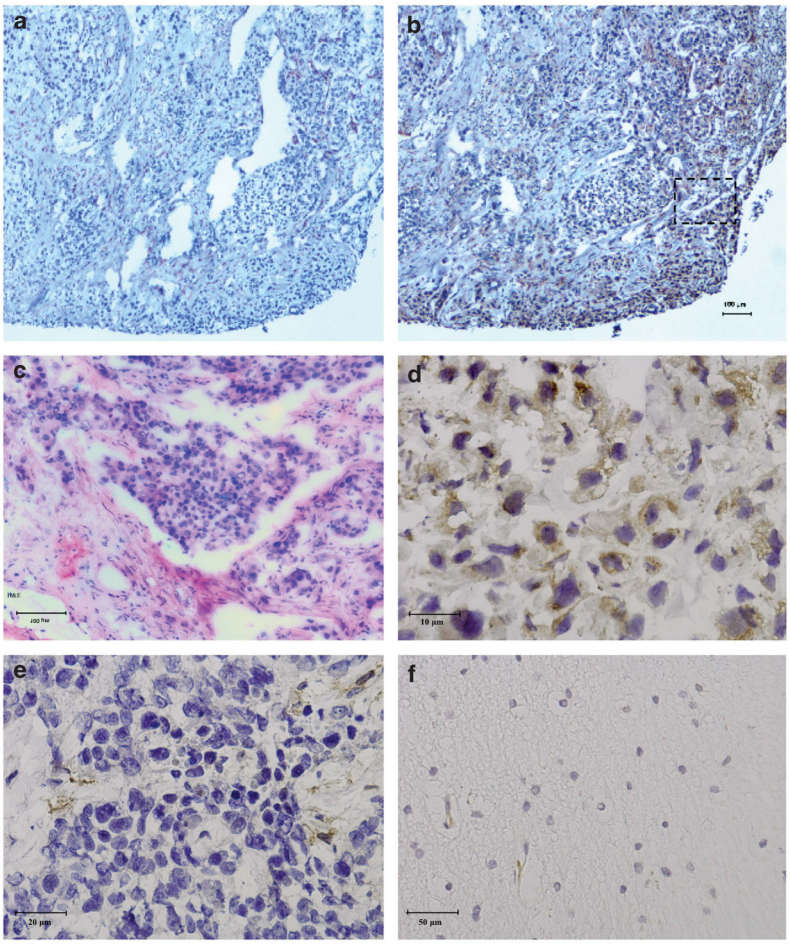

Figure 2.

Detection of NT-3 protein in brain metastases from breast cancer patients. (**a**) × 100 magnification of the brain metastasis tissue section with the isotype-matched negative control antibody staining. (**b**) ×100 magnification of the brain metastasis tissue section with the NT-3 antibody staining. (**c**) ×200 magnification of the brain metastasis tissue section with the hematoxylin and eosin (H&E) staining. (**d**) ×400 magnification of the brain metastasis tissue section stained with the NT-3 antibody. (**e**) ×400 magnification of the primary breast tumor tissue section stained with the NT-3 antibody. (**f**) ×200 magnification of the normal brain section stained with the NT-3 antibody.

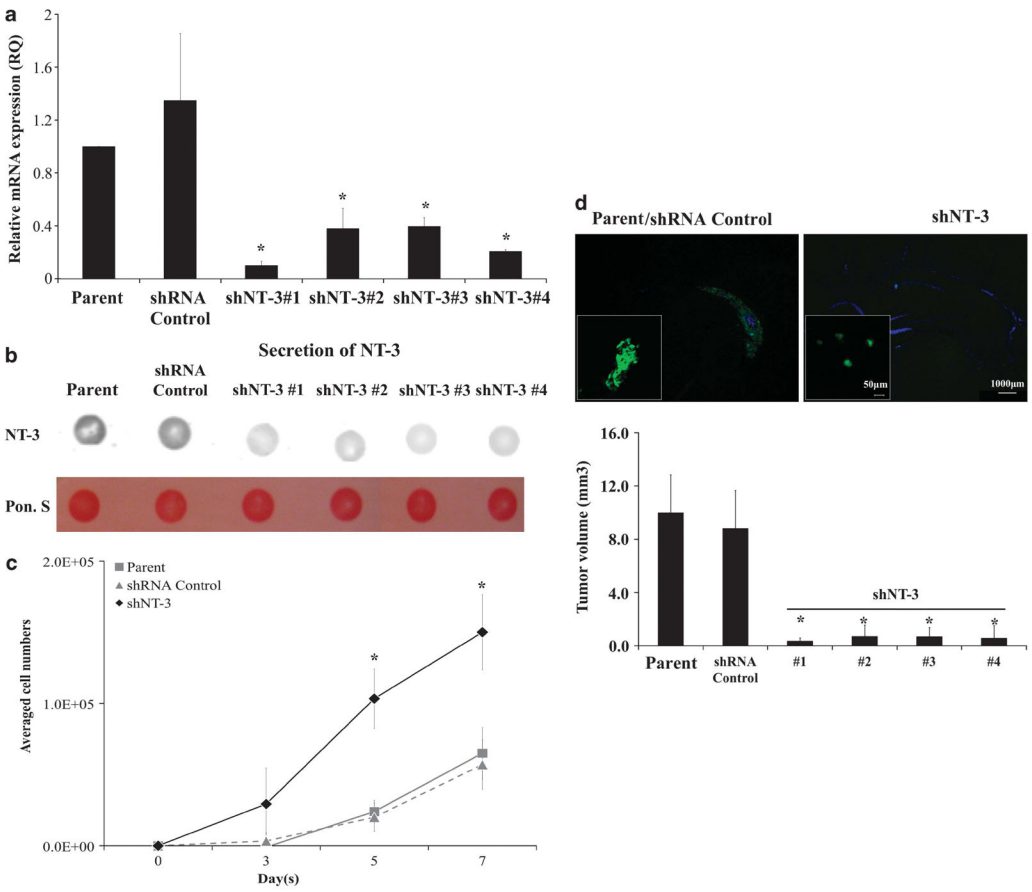

Figure 3.

Reduced NT-3 expression in brain selective breast cancer cells increase cell proliferation *in vitro* but decrease the metastatic growth of these cells *in vivo*. (**a**) mRNA expression of NT-3 in MDA-MB 361 breast cancer cells without transfection (Parent), transfected with scramble shRNA (shRNA Control), and transfected with shRNAs against NT-3 (shNT-3 nos. 1–4). (**b**) Dot blot analysis of NT-3 protein in the condition media. (**c**) Proliferation of cells with or without shNT-3. (**d**) Representative images and tumor volumes of metastatic brain lesions derived from cells transfected with shRNA control (left) or the shRNA against NT-3 (right; $n = 6$ in each group). *Statistically significant values ($P<0.05$).

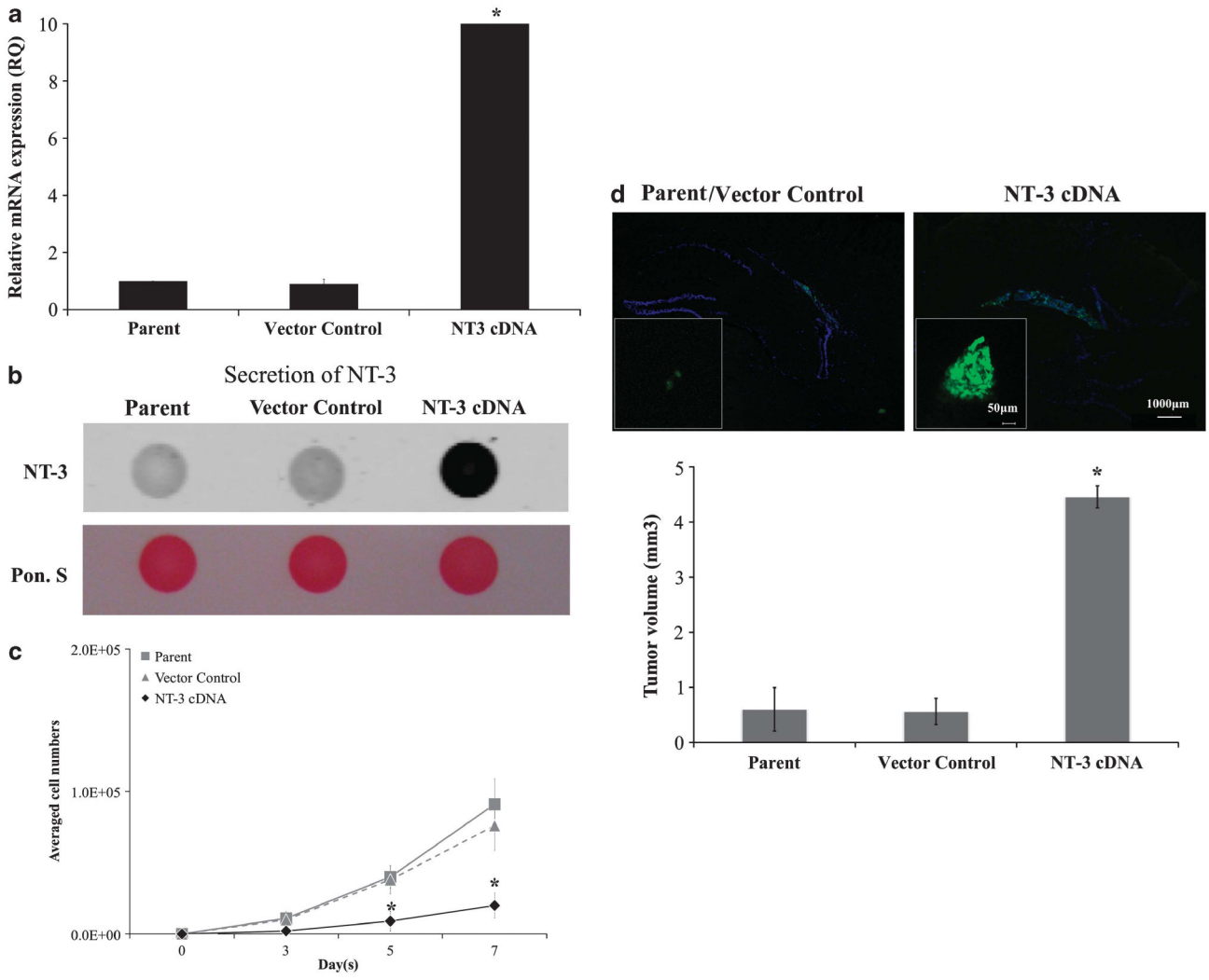

Figure 4.

Increased NT-3 expression in non-brain selective breast cancer cells decrease cell proliferation *in vitro* but increase the metastatic growth of these cells *in vivo*. (**a**) mRNA expression of NT-3 in MDA-MB 231 breast cancer cells without transfection (Parent), transfected with an empty vector (Vector Control) and transfected with NT-3 cDNA (NT-3 cDNA). (**b**) Dot blot analysis of NT-3 protein in the condition media. (**c**) Proliferation of cells with or without overexpressing NT-3 cDNA. (**d**) Representative images and tumor volumes of metastatic brain lesions derived from cells transfected with an empty vector (left) or the NT-3 cDNA (right) (n = 6 in each group). *Statistically significant values (P<0.05).

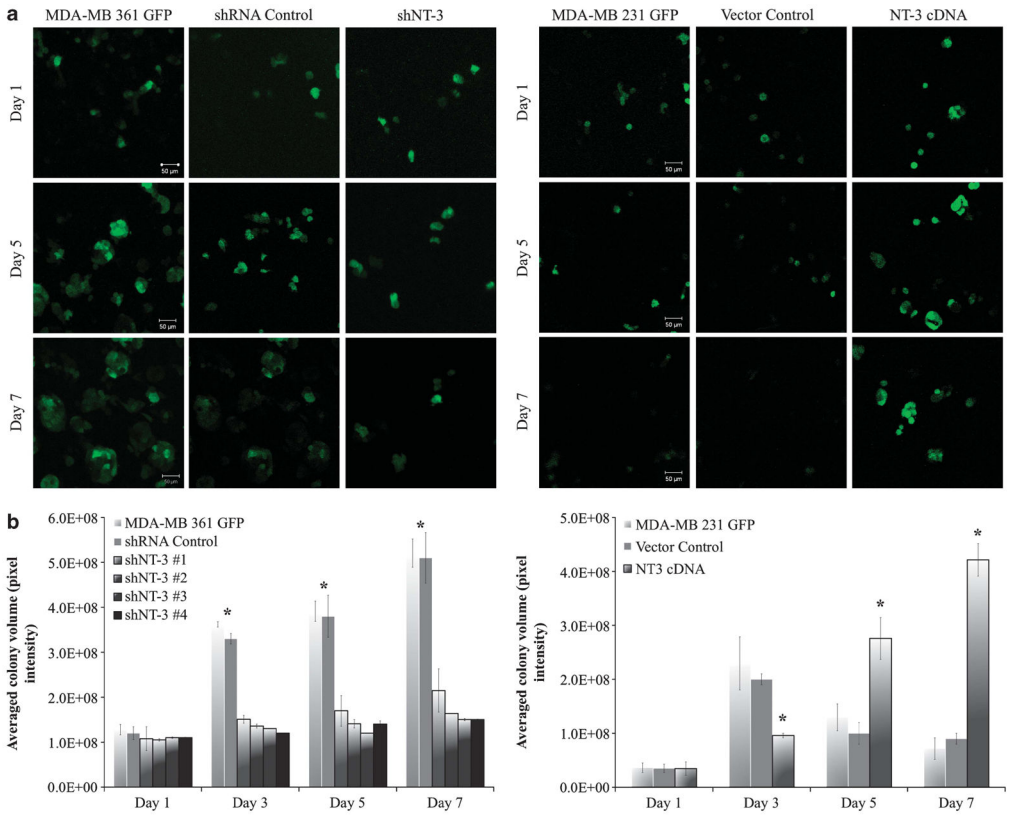

Figure 5.

Organotypic cultures of metastatic breast cancer cells. (**a**) Colonization of metastatic breast cancer cells with endogenous NT-3 or transfected with shNT-3 or NT-3 cDNA on organotypic brain slice cultures. Green fluorescence proteins expressed in the cells were used to visualize the colony formation and quantify the growth of the colonies using the scanning confocal microscope. (**b**) Quantification of GFP colonies by NIH ImageJ software at different time points. *Statistically significant values (P<0.05).

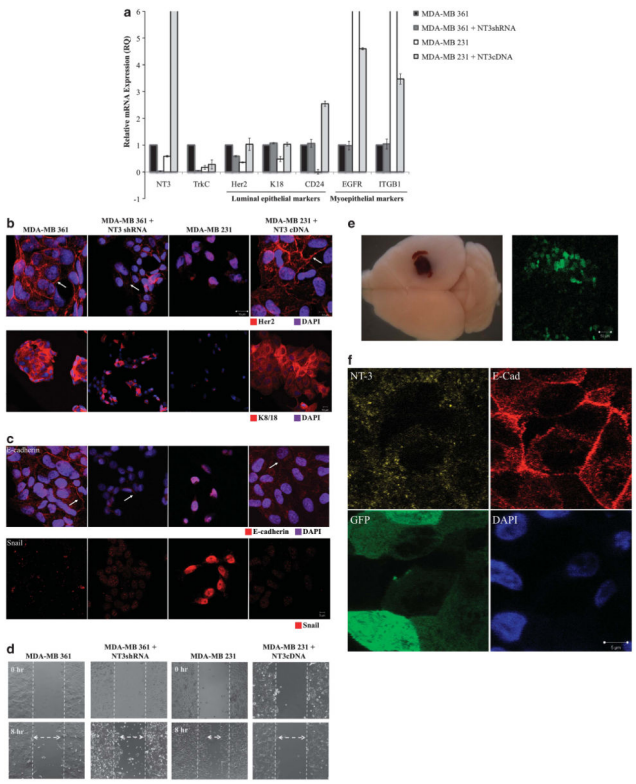

Figure 6.

Genetic, morphological and functional changes of metastatic breast cancer cells with increased or decreased NT-3 expression. (**a**) Relative mRNA changes of luminal and myoepithelial markers in brain selective breast cancer cells (MDA-MB 361 and MDA-MB 231 + NT-3 cDNA) and non-brain selective breast cancer cells (MDA-MB 231 and MDA-MB 361 + NT-3shRNA). (**b**) Immunostaining of HER2 and Keratin8/ 18 in the metastatic lesions of brains implanted with either brain selective or non-brain selective breast cancer cells. (**c**) Immunostaining of E-cadherin and Snail in the metastatic lesions of brains implanted with either brain selective or non-brain selective breast cancer cells. (**d**) Wound-healing assay to evaluate the migratory ability of brain selective and non-brain selective breast cancer cells. (**e**) A representative gross image of spontaneous brain metastasis with disruption of blood–brain barrier (left panel) and a confocal image of brain metastasis GFP colonies in a brain section (right panel). (**f**) Immunostaining of NT-3 and E-cadherin in lesions of spontaneous brain metastasis. The stem-like subpopulation was engineered to express GFP for visualization.

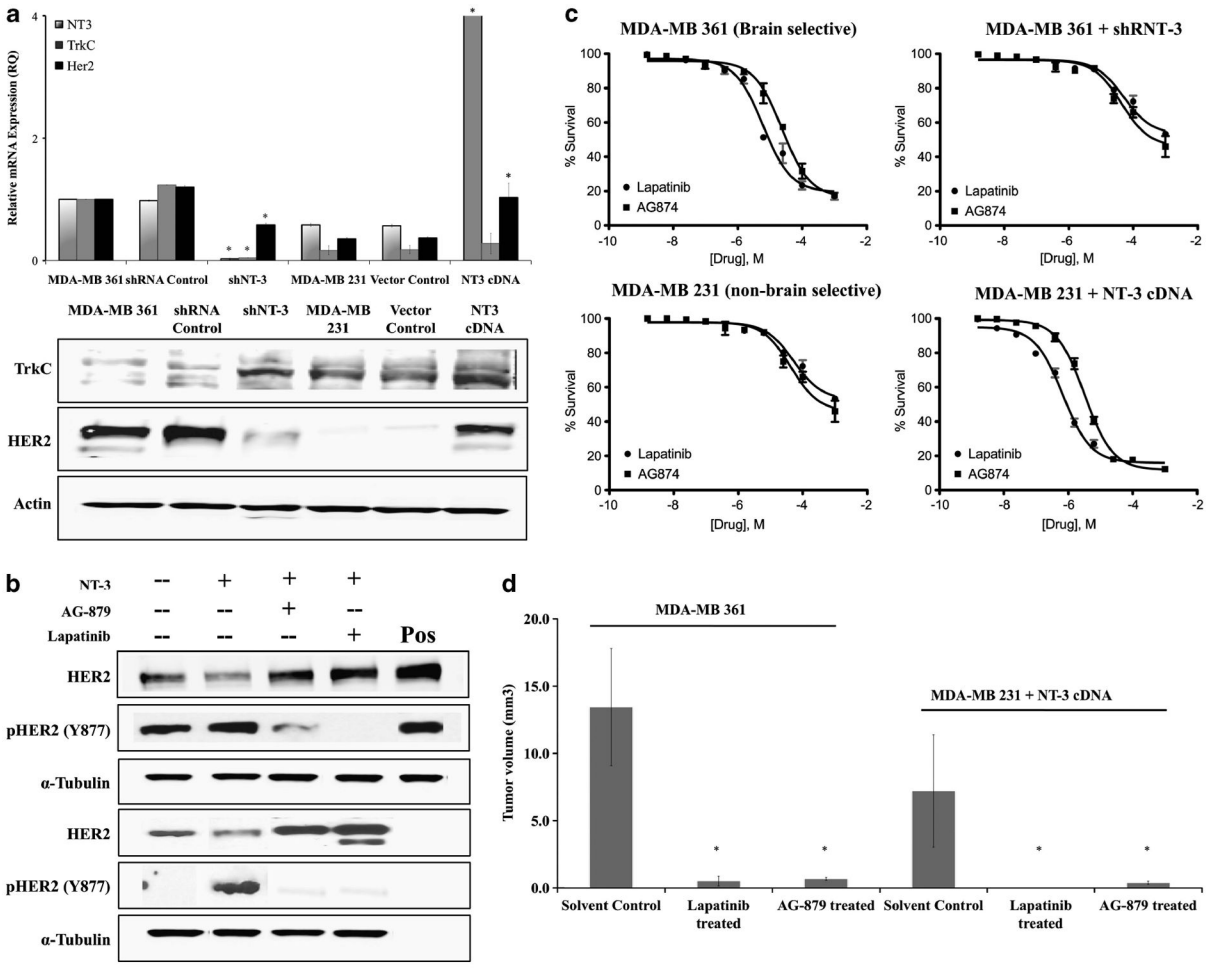

Figure 7.

HER2 inhibitors are effective in suppressing HER2 phosphorylation of brain selective and non-brain selective breast cancer cells *in vitro* and reducing the metastatic of these cells *in vivo*. (**a**) Changes of TrkC (NT-3 high-affinity receptor) and HER2 mRNA and protein levels in brain selective and non-brain selective breast cancer cells. (**b**) Western blot analysis of total HER2 and phosphorylated HER2 (Y877) in the presence of exogenous NT-3 with or without the HER2 small-molecule inhibitors (Lapatinib and AG874). (**c**) Dose-response curve of brain selective and non-brain selective breast cancer cells against HER2 small-molecule inhibitors. (**d**) Changes in metastatic growth of brain selective breast cancer cells *in vivo* after the Lapatinib and AG874 treatments. *Statistically significant values (P<0.05).

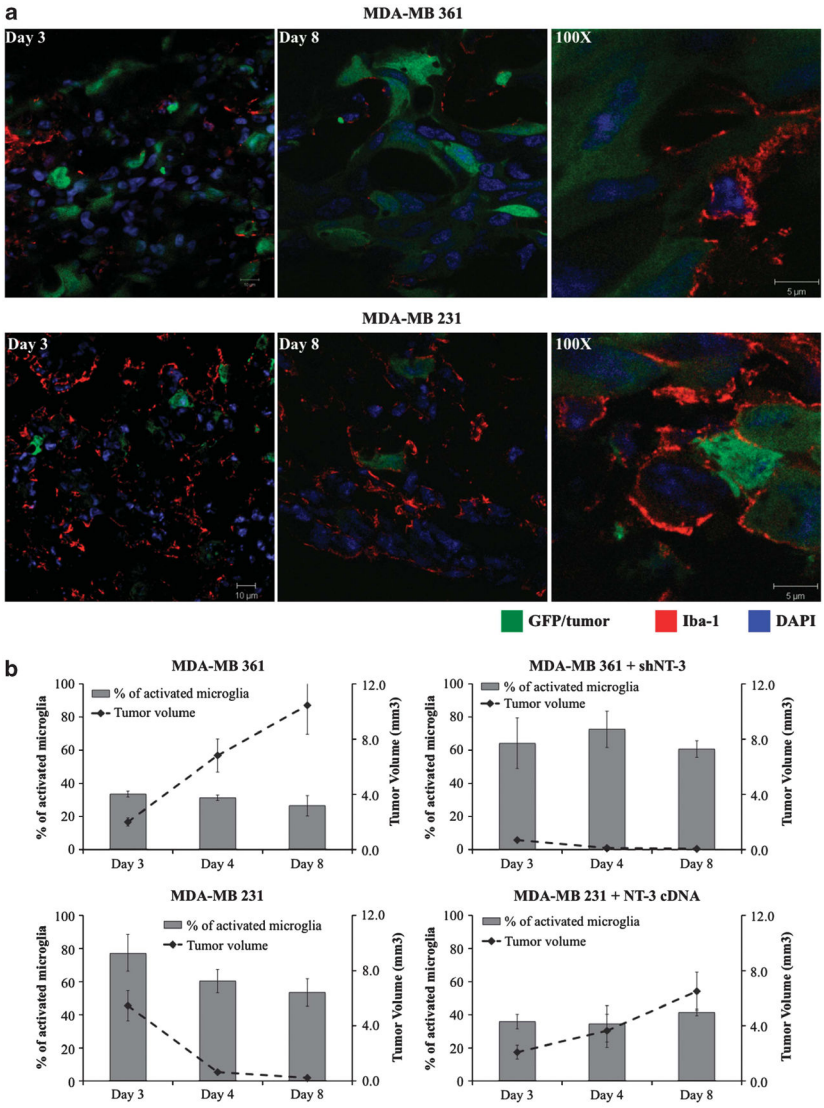

Figure 8.

Microglia activation in the metastatic lesions of breast cancer cells *in vivo*. (**a**) Staining of microglia surrounding and infiltrating the metastatic lesions derived from brain selective and non-brain selective breast cancer cells. Iba-1 staining was used to visualize activated microglia. (**b**) Quantifications of the percentage of activated microglia and tumor volumes in the metastatic lesions derived from brain selective and non-brain selective breast cancer cells.